JACS
JOURNAL OF THE AMERICAN CHEMICAL SOCIETY

Article

pubs.acs.org/JACS

A Multi-State, Allosterically-Regulated Molecular Receptor With Switchable Selectivity

Jose Mendez-Arroyo,[†] Joaquín Barroso-Flores,[§] Alejo M. Lifschitz,[†] Amy A. Sarjeant,[†] Charlotte L. Stern,[†] and Chad A. Mirkin*[,†]

[†]Department of Chemistry and International Institute for Nanotechnology, Northwestern University, 2145 Sheridan Road, Evanston, Illinois 60208, United States

[§]Centro Conjunto de Investigación en Química Sustentable, UAEM-UNAM, Carretera Toluca-Atlacomulco Km 14.5, Unidad San Cayetano, Toluca, Estado de México C. P. 50200, México

Supporting Information

ABSTRACT: A biomimetic, ion-regulated molecular receptor was synthesized via the Weak-Link Approach (WLA). This structure features both a calix[4]arene moiety which serves as a molecular recognition unit and an activity regulator composed of hemilabile phosphine alkyl thioether ligands (P,S) chelated to a Pt(II) center. The host−guest properties of the ion-regulated receptor were found to be highly dependent upon the coordination of the Pt(II) center, which is controlled through the reversible coordination of small molecule effectors. The environment at the regulatory site dictates the charge and the structural conformation of the entire assembly resulting in three accessible binding configurations: one closed, inactive state and two open, active states. One of the active states, the semiopen state, recognizes a neutral guest molecule, while the other, the fully open state, recognizes a cationic guest molecule. Job plots and ^{1}H NMR spectroscopy titrations were used to study the formation of these inclusion complexes, the receptor binding modes, and the receptor binding affinities (K_a) in solution. Single crystal X-ray diffraction studies provided insight into the solid-state structures of the receptor when complexed with each guest molecule. The dipole moments and electrostatic potential maps of the structures were generated via DFT calculations at the B97D/LANL2DZ level of theory. Finally, we describe the reversible capture and release of guests by switching the receptor between the closed and semiopen configurations via elemental anion and small molecule effectors.

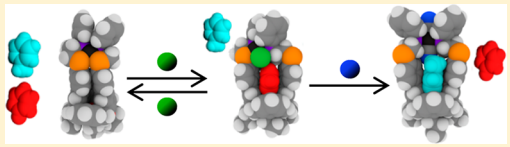

INTRODUCTION

Allosteric control of binding sites in proteins and enzymes plays a major role in the regulation of a diverse array of critical biological processes, such as protein folding[1] and oxygen transport.[2] Enzymatic activity in these processes is often regulated either by controlling the steric profile or the chemical affinity of the binding site for different substrates.[3] The former type of allosteric control is commonly employed to regulate physical access to a binding site, as in the case of protein folding in molecular chaperonins, thus enabling toggling between an active and an inactive state.[4−6] In contrast, the switching between multiple and distinct active states requires the ability to control the chemical affinity of the reactive cavity for a variety of guests without hindering the substrates' access to it. As such, changes in pH and their associated effects on the structure of hemoglobin are used to regulate the binding of oxygen and carbon dioxide by the same protein, providing an efficient mechanism for the control of gas concentrations in biological tissues.[7,8]

In order to mimic the properties and regulatory capabilities of reactive cavities in biological machinery, a number of abiotic counterparts have been developed in which the steric profile and the size of molecular cages are regulated via pH changes,[9−12] photochemistry,[13−16] redox processes,[17−19] and coordination chemistry.[20−30] Such abiotic systems have exhibited the ability to encapsulate and release small organics,[31] therapeutic agents,[32] and biomolecules[33] as a response to changing chemical environment. While the applications of such structures in phase transfer catalysis,[34−36] drug delivery,[37] and sensing[38] have been reported, the usefulness of this approach could be greatly expanded through the development of an abiotic platform to allosterically toggle a single cavitand between an inactive and multiple active states with different recognition properties. However, controlling molecular capsules through this approach remains a significant challenge, since regulation must then involve several chemical and structural transformations around the cavitand that must be orthogonal to one another.

Herein, we report the synthesis of a novel calix[4]arene ion-regulated receptor assembly whose encapsulation properties can be modulated via small molecule displacement reactions of hemilabile ligands coordinated to d^8 metal centers strategically positioned above the cavitand (Scheme 1). Our design is based on the Weak-Link Approach (WLA)[25,39−41] to the synthesis of supramolecular structures, which has been previously used to construct abiotic allosteric enzyme mimics with applications in sensing,[42,43] signal amplification,[24] and control of catalytic

Received: April 14, 2014
Published: July 9, 2014

   dx.doi.org/10.1021/ja503506a | J. Am. Chem. Soc. 2014, 136, 10340−10348

Scheme 1. Allosteric Modulation of Calix[4]arene Ion-regulated Receptor Assemblies via the WLA

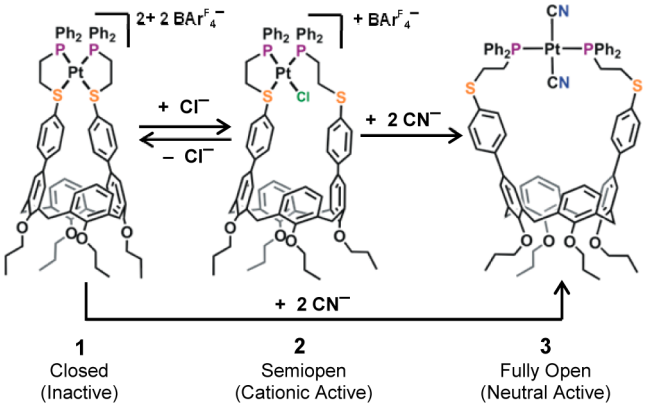

activity.[44] In the present work we demonstrate that the size and charge of a WLA ion-regulated receptor assembly can be modulated using small molecule effectors, thus enabling access to three exclusive supramolecular configurations, each with unique host–guest properties. In particular, this system features a physically blocked inactive state and two unique active states that display similar cavity sizes while showing distinct chemical affinity for different types of guest molecules. The characteristics of each receptor binding state (**1**, **2**, or **3**) are determined by the coordination modes of the hemilabile moieties extending from the cavitand and the associated electrostatic characteristics of the cavity, all of which are regulated with molecular effectors (Cl^- and CN^-). The combined control of both cavity size and chemical affinity in this coordination-controlled assembly makes use of the most prevalent mechanisms of allosteric regulation found in biological machinery and offers a promising strategy to the development of biomimetic supramolecular assemblies.

RESULTS AND DISCUSSION

Synthesis. Calix[4]arenes are commonly studied molecules whose host–guest properties can be synthetically adjusted via transformations on the cavitand's upper and lower rims.[45−47] Generally, modifications of the upper rim result in extension of the cavitand's depth and lead to higher binding affinities for certain aromatic guests.[45−48] For this reason, it was hypothesized that bifunctionalization of calix[4]arene in the 5 and 17 positions with hemilabile phosphine-alkyl thioether (P,S) moieties through phenyl spacers would create a high-affinity binding pocket suitable for small aromatic guests. The synthesis of compound **4** was thus achieved via a convergent process in 8 steps from commercially available calix[4]arene tetrol (**7**) (Scheme 2). In order to preserve the integrity and flexibility of the binding site throughout coordination chemistry transformations, the calix[4]arene was first locked in a cup conformation through tetraalkylation of the lower rim. This transformation was followed by halogenation with *N*-bromosuccinimide to incorporate four bromide units along the calix[4]arene's upper rim. Symmetric debromination of two of these four brominated positions was achieved via selective lithiation with 2 equiv of *n*-butyl lithium and quenching with methanol. The remaining brominated moieties were coupled to sulfide protected P,S ligands via Pd catalyzed cross-coupling. Finally, removal of the protecting sulfide in compound **11** was achieved via reaction with Schwartz's reagent to yield the air-sensitive hemilabile ligand **4** in 14% overall yield.

Assembly of the Pt(II)-containing ion-regulated receptor system **1** was achieved following well-established WLA protocols.[39−41] Addition of a dichloro Pt(II) precursor to compound **4** in dichloromethane yields a mixture of Pt(II)-containing species in which the Cl^- anions are dynamically exchanging in and out of the inner coordination sphere, partially displacing the P,S moieties. Both chlorides can be abstracted from the inner coordination sphere through either an increase in solvent polarity (addition of methanol), precipitation of Cl^- from solution, or via displacement with strongly coordinating anions. In particular, abstraction of 1 or 2

Scheme 2. Synthesis of Calix[4]arene Functionalized Hemilabile Ligand 4

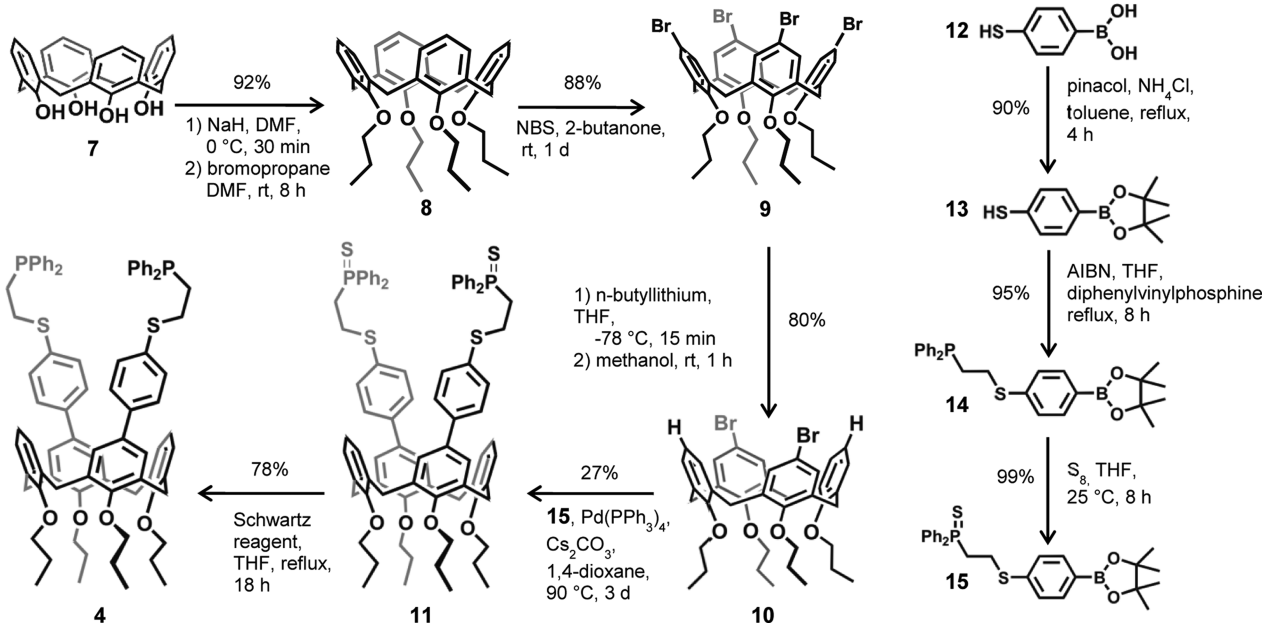

dx.doi.org/10.1021/ja503506a | J. Am. Chem. Soc. 2014, 136, 10340−10348

equiv of Cl^- using stoichiometric amounts of $NaBAr^F{}_4$ yields semiopen complex **2** or closed complex **1**, respectively, in quantitative yield. Closed complex **1** can be in turn converted to semiopen complex **2** and fully open complex **3** via addition of 1 equiv of Cl^- or 2 equiv of CN^-, respectively (Scheme 1). Although complexes **1** and **3** are stable in solution and exist as well-defined entities, the ion-regulated receptor **2** displays a fast dynamic exchange in solution in which the two thioether linkages compete for coordination with Pt(II), alternating between bound and displaced states. This fluxional process commonly occurs in WLA systems when the coordination strength of two thioether linkages is similar, and it has been extensively documented in the literature.[41,49,50] A complete account of synthetic procedures and associated characterization data (^{1}H NMR, ^{31}P{^{1}H}NMR, and ESI-MS) of compounds **4** and **8**–**15** can be found in the Supporting Information.

Formation of Inclusion Complexes. N-substituted pyridine derivatives are a diverse class of electron-deficient, aromatic compounds that are well-known to form inclusion complexes with functionalized calix[4]arenes.[51−54] Two guests, cationic *N*-methylpyridinium $BAr^F{}_4^-$ (**5**) and neutral *N*-oxide pyridine (**6**), were thus selected in order to probe the binding properties of molecular receptors **1**–**3**. Formation of inclusion complexes was determined by ^{1}H NMR titration of guests **5** and **6** into solutions of complexes **1**–**3** (Figure 1). The binding stoichiometry of host–guest complexes was determined by using Job plots (see Supporting Information). In the case of cationic guest **5**, ^{1}H NMR titration displays no significant

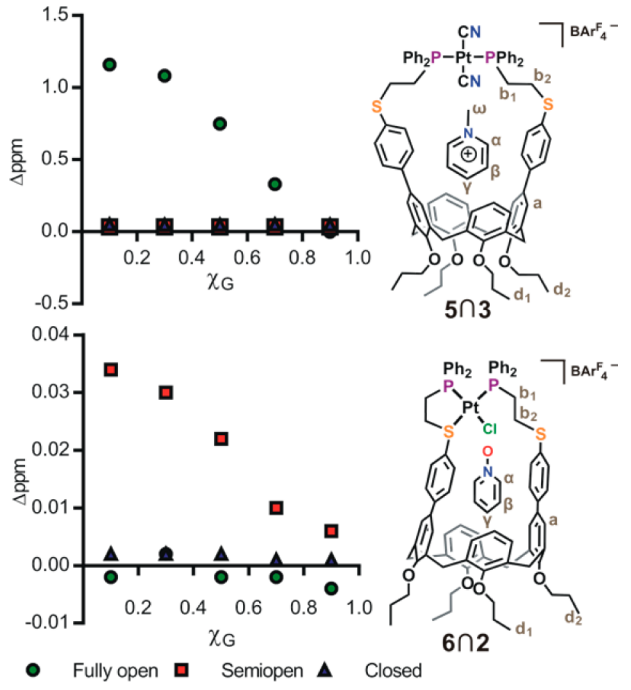

Figure 1. ^{1}H NMR traces for ion-regulated receptor assemblies **1**–**3** and their corresponding inclusion complexes. All titrations were performed at room temperature with a total concentration of host and guest of 30 mM in CD_3CN, except for fully open complex **3**, which was studied in CD_2Cl_2 due to poor solubility in CD_3CN. Note that receptor **2**, when dissolved in CD_2Cl_2 does not form an inclusion complex with **5**, ruling out the difference between **2** and **3** being purely a solvent effect. The ^{1}H NMR resonances of the *N*-methyl group (ω) were used as a probe for **5**, and in titrations involving **6** the resonance of the β proton was used.

interaction with the molecular receptor in the closed complex **1** or semiopen complex **2** (Figure 1). While the lack of binding affinity of **5** for closed complex **1** is understandable, based on the reduced cavity size that the coordination mode imparts on the calix[4]arene, the same behavior in the semiopen complex **2** suggests that the WLA can be exploited to alter the intrinsic affinity of calix[4]arene receptors for electron-deficient guests. Indeed, the lack of encapsulation found in **2** can be attributed to the electrostatic repulsion between the Pt(II) regulatory site and the cationic guest **5**. Accordingly, the formation of a 1:1 host–guest complex can only be observed between cationic guest **5** and the molecular receptor in its neutral, fully open configuration **3**, indicating that the electrostatic repulsion between **5** and **2** plays a major role dictating the host–guest selectivity. Neutral guest **6**, on the other hand, does not form any detectable inclusion complexes with fully open receptor **3**, only very small changes in the chemical shift of guest molecule **6** are observed. Only the positively charged semiopen complex **2** is able to encapsulate guest molecule **6** in the form of a 1:1 inclusion complex (Figure 1). Closed complex **2** does not incorporate **6**, presumably due to the collapse of the binding cavity and steric inaccessibility. Taken together, the ability to regulate the recognition of guest molecules **5** and **6**, simply by adjusting the size and charge of the host pocket using discrete ion-driven reactions, underscores how the WLA can be used to create multi-state molecular receptors that can be addressed via well-defined chemical events.

^{1}H NMR Titrations and Solution Behavior. Structural rearrangement of **2** and **3** upon formation of complexes **6**∩**2** and **5**∩**3** was investigated by tracking changes in ^{1}H NMR spectroscopy resonances through the titration of **6** and **5** into CD_3CN and CD_2Cl_2 solutions of **2** and **3**, respectively. From these data, the binding affinities (K_a) and binding modes of guests **5** and **6** for their respective hosts **3** and **2** were elucidated. Figure 2 shows the ^{1}H NMR spectra resulting from the addition of up to 18 equiv of **5** to receptor **3**. The signals assigned to *N*-methyl protons (ω) in **5** exhibit a characteristic large upfield shift upon cavitand encapsulation of guest.[45,46] Upfield chemical shifts of the α, β, and γ protons in **5** are also observed, suggesting that the entire guest molecule is in the cavity.[45−48,51−53] Furthermore, the binding of **5** by ion-regulated receptor **3** also reveals general structural reorganization of the assembly upon encapsulation, resulting in chemical changes in the chemical shift of the proton resonances corresponding to the P,S ligands and the calix[4]arene. In particular, the ethyl protons (b_1,b_2) in the P,S ligands, which appear as broad features prior to guest incorporation, are split into two distinct triplets. This splitting suggests reduced mobility of the flexible ethyl bridge and stabilization into an overall more rigid conformation. Accordingly, the two sets of signals from methyl protons at the end tail of the propyl chains (d_1,d_2) in the calix[4]arene bottom rim coalesce into a broad triplet. This phenomenon is attributed to the reduction in anisotropy of the calix[4]arene cup to achieve a more uniform conformation that allows for a larger volume, which can accommodate the guest.

Similar effects on ^{1}H NMR resonances are observed upon titration of 32 equiv of **6** into a solution of **2** (Figure 2). In particular, the aromatic protons in **6** are also shifted upfield, as in the case of host–guest complex **5**∩**3**, suggesting the inclusion inside the cavity of **2**. The broad signals of the ethyl spacers (b_1,b_2) of the P,S ligands in **2** also undergo a process of rearrangement with increasing concentrations of **6**.

dx.doi.org/10.1021/ja503506a | J. Am. Chem. Soc. 2014, 136, 10340−10348

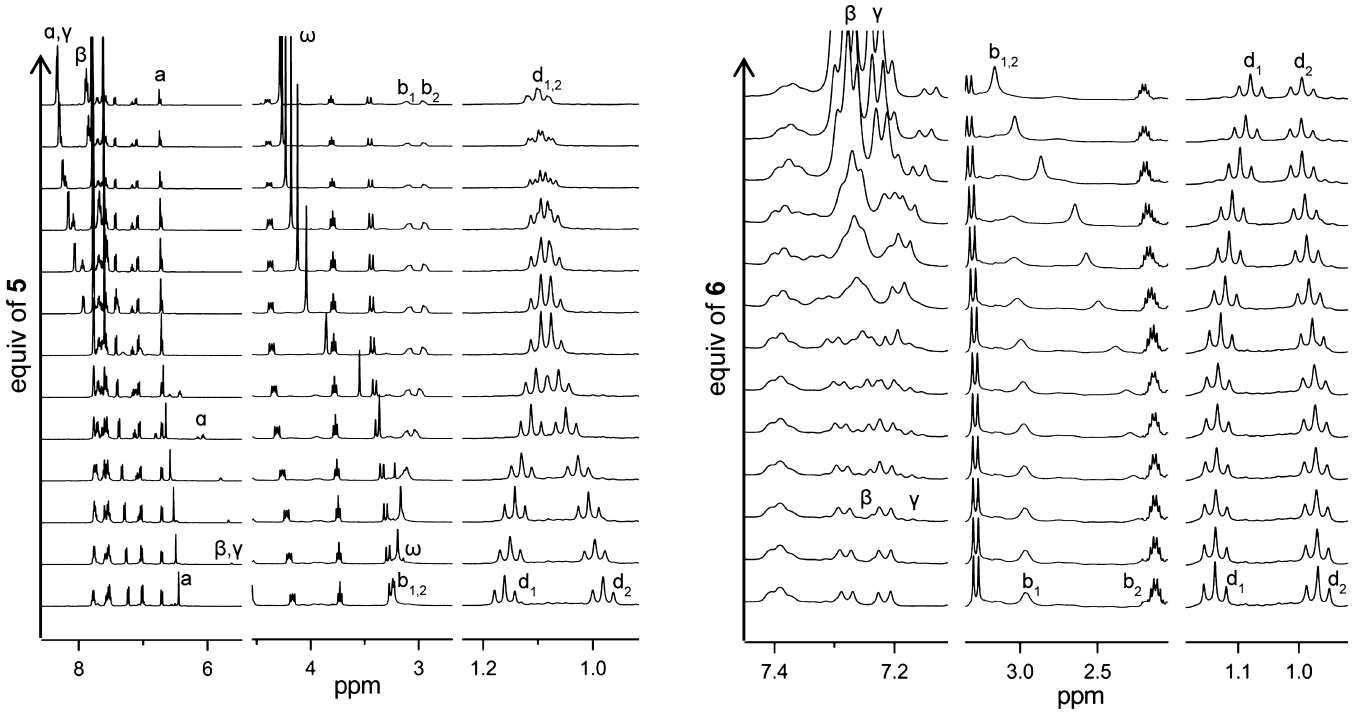

Figure 2. (Left) ^{1}H NMR titration of guest **5** (18 equiv) into ion-regulated receptor **3**. Titration was performed at room temperature with a host concentration of 26 mM in CD_2Cl_2. (Right) ^{1}H NMR titration of guest **6** (32 equiv) into ion-regulated receptor **2**. Titration was performed at room temperature with a host concentration of 30 mM in CD_3CN.

This is seen in the downfield shift and coalescence of these ethyl ^{1}H NMR signals into a single broad resonance at high guest concentrations. Furthermore, as in the case of the **5∩3** complex, the resonances for the methyl tail in the propyl chains (d_1,d_2) of **2** also show the same coalescing trend, suggesting that inclusion of **6** imparts a change in the shape of the flexible calix[4]arene cup. The binding affinities determined via ^{1}H NMR titrations above are shown in Table 1. In both cases, **5∩3** and **6∩2** complexes, the resonance in the host (Table 1) displays the greatest shift and the least overlap with other resonances and therefore was used to calculate the guest binding affinity. In complex **6∩2**, the most notable changes in the ^{1}H NMR spectra upon encapsulation occur in the aromatic region, to the signal corresponding to the (β) hydrogen signal in **6**. In both cases the aromatic signals of the hosts show smaller but significant shifts. The binding affinities of **5** for **3** are within the expected magnitude range for similar calix[4]arenes host–guest systems that rely solely on cation–π based interactions (<1000 M^{-1} for calix[4]arenes with *N*-methylpyridinium salts).[45−48,51−53,55] Similarly, the determined binding affinity of **6** for **2** is comparable to other previously reported calix[4]arene host guest systems involving neutral guests (<200 M^{-1}).[45−48,51−53,56,57]

Table 1. Binding Affinities of Inclusion Complexes

guest	host	K_a	solvent	Δppm
5	**3**	691 ± 99	CD_2Cl_2[a]	0.30
6	**2**	3.3 ± 0.4	CD_3CN[b]	0.21

[a] **3** is not soluble in any appreciable amount in CD_3CN. [b] **6** in CD_2Cl_2 is non-innocent and reacts with **2** to decompose the complex. Comparisons between the K_a values obtained in different solvents must be treated with caution due to the different stabilization provided by each solvent.

Solid-State Characterization of Host–Guest Complexes. Single crystals suitable for X-ray diffraction of **1**, **6∩2**, and **5∩3** were grown to gain further insight into the structural features of the three ion-receptor configurations and their respective host–guest complexes. The solid-state structure of **1** confirms that both P,S ligands chelate to the Pt(II) metal center in a square planar coordination geometry causing the collapse of the calix[4]arene cavity (Figure 3). In particular, the distance between the centroids of the two phenyl groups extending from the P,S ligands is 3.668 Å, which physically prevents complex **1** from engaging in host–guest interactions, since the distance lies within the range of π–π stacking. Furthermore, this closed configuration forces the distortion of the flexible calix[4]arene upper rim into an ellipsoid that is approximately 7.718 by 4.784 Å. The disorder of the lower-rim propyl tails observed in the solid-state structure arises from the multiple orientations the alkyl tails can adopt in the face-on arrangement found in solid-state structure of **1**.

The solid-state structure of **6∩2** displays a coordination environment around Pt(II) corresponding to a semiopen configuration, in which only one P,S moiety is fully chelated, and the remaining two coordination sites are occupied solely by monodentate P-bound hemilabile ligand and Cl^- (Figure 4). Upon complexation of **6** by **2**, the mondentate P-bound hemilabile moiety of **2** extends outward in order to incorporate the guest. Indeed, the total distance between phenyl spacers attached to the P,S ligands is 7.392 Å, allowing enough space for an aromatic guest such as **6** to fit snuggly within the cavity and remain bound through π–π stacking interactions. Interestingly, guest molecule **6** does not reside at the center of the cavity but is instead 0.349 Å closer to the phenyl ring attached to the nonchelating P,S ligand, as compared to the chelated one. This interaction between **6** and the monodentate P-bound hemilabile ligand reduces the dihedral angle between

dx.doi.org/10.1021/ja503506a | J. Am. Chem. Soc. 2014, 136, 10340−10348

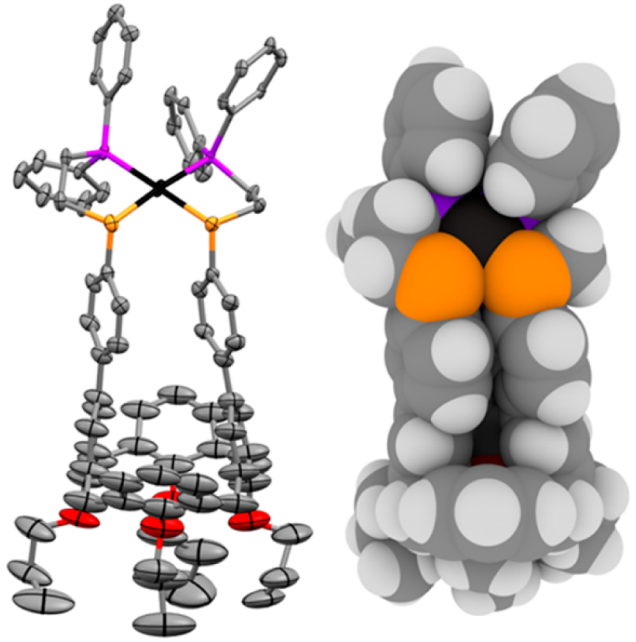

Figure 3. (Left) Solid-state structure of **1** drawn with 30% probability thermal ellipsoids. Counterions and solvent molecules are omitted for clarity. (Right) Space-filling representation of **1** showing the physically blocked cavity by the $\pi-\pi$ interaction between the two phenyl rings extending from the P,S ligands. Color scheme for the atoms: platinum, black; sulfur, yellow; phosphorus, magenta; oxygen, red; carbon, gray; hydrogen, white.

the P-bound ligand's phenyl spacer and the calix[4]arene to 12.03°, compared to dihedral angles of 26.42° observed for the phenyl spacer in the P,S chelated ligand. In addition to $\pi-\pi$ stacking, the alignment of **6** inside **2** suggests an electrostatic interaction between the negatively charged oxygen in **6** and the cationic Pt(II) in **2**. Although the Pt···O distance (6.421 Å) is too long for a bonding interaction, the dipole interaction between the O atom in **6** and the positively charged Pt(II) center is strong enough to direct the orientation of **6** when incorporated inside **2**. Furthermore, the incorporation of **6** into **2** also seems to reduce the anisotropy of the calix[4]arene upper rim into a more circular ellipsoid measuring 7.230 by 5.945 Å, which is consistent with the observations made via ^{1}H NMR spectroscopy.

In the solid-state structure of **5**∩**3** (Figure 4), the phosphine groups bound to the Pt(II) metal center display a *trans* conformation, as opposed to complexes **1** and **2** in which the phosphine moieties are *cis* to one other. This coordination geometry is a result of the large *trans* effect of the two cyanides, forcing the P,S ligands far away from each other, largely expanding the cavity in the supramolecular framework. Although ion-regulated receptor **3** is theoretically flexible enough for the phenyl spacers to reach distances of over ∼10 Å from phenyl to phenyl, the solid-state structure shows that the distances between ligands is only 7.635 Å. This occurs because the receptor **3** adapts its cavity size to create the most appropriate binding environment for guest **5**. As in the case of **6**∩**2**, guest **5** is located closer to one of the P,S ligands, rather than being located symmetrically at the center of the cavity. The dihedral angle between the phenyl spacer closest to the guest and the calix[4]arene is decreased to 1°, presumably allowing the guest to engage in stronger face-on $\pi-\pi$ interactions. As opposed to the **6**∩**2** host–guest complex, in

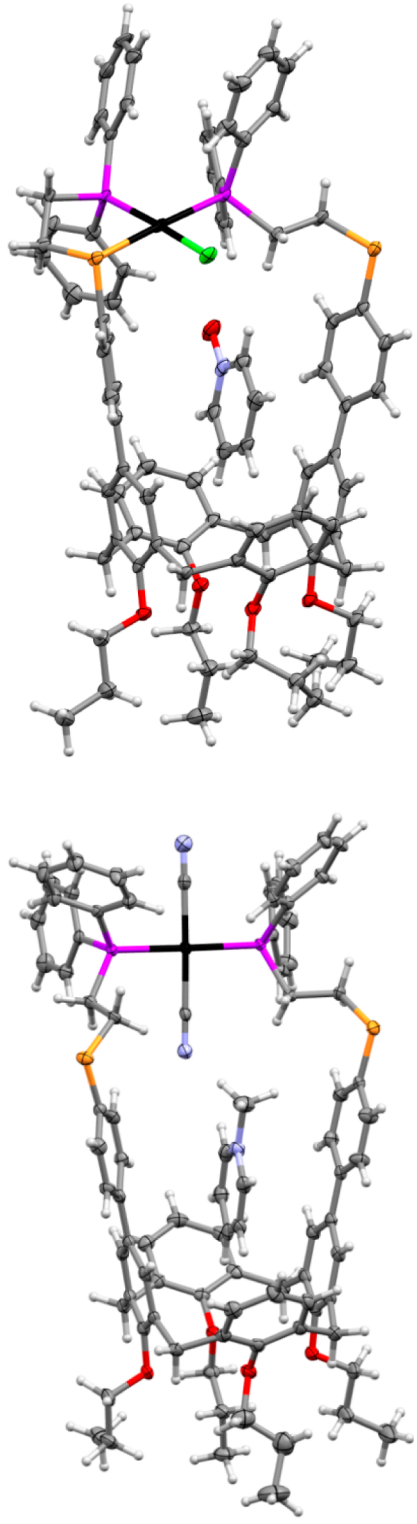

Figure 4. (Top) Solid-state structure of **6**∩**2** drawn with 50% probability thermal ellipsoids. (Bottom) Solid-state structure of **5**∩**3** drawn with 50% probability thermal ellipsoids. $BAr^{F}{}_{4}^{-}$ counterions and solvent molecules are omitted for clarity. Color scheme for the atoms: platinum, black; sulfur, yellow; nitrogen; blue; chloride, green; phosphorus, magenta; oxygen, red; carbon, gray; hydrogen, white.

which the dipole–cation interaction plays a major role in the alignment of the guest inside the cavity, sterics seem to play a more significant role in the orientation of **5** upon inclusion in **3**. The Pt(II) center is positioned away from the cavity, and the

dx.doi.org/10.1021/ja503506a | J. Am. Chem. Soc. 2014, 136, 10340–10348

N-methyl group in **5** is located in such a fashion that allows for a short contact (2.380 Å) between the CN^- ligand and the *N*-methyl protons. Furthermore, **5** lays lower in the calix[4]arene cavity, as compared to **6∩2**, suggesting a higher contribution of cation-π interactions to the formation of the inclusion complex.

In Situ Allosteric Regulation of Host–Guest Properties. The quantitative and reversible coordination chemistry-induced transformation between complexes **1**–**2** and the parallel formation of host–guest complex **6∩2** was studied in tandem to probe the potential for in situ control of host–guest properties of the present ion-regulated receptor system. This was accomplished via the regulation of the Pt(II) coordination environment by sequential addition and abstraction of Cl^- in a CD_3CN solution containing **6**. The solid-state structure of **1** shows no guest binding can occur in the closed configuration, and Job plots data are consistent with this conclusion for **1** dissolved in CD_3CN. Indeed, the ^1H NMR chemical shift values for the resonances for **6** in the presence of **1** are identical to those for free guest in solution (Figure 5). On the other hand, the ^1H NMR data clearly show the formation of an inclusion complex with **6** when **1** is transformed into semiopen complex **2**. Abstraction of Cl^- from **2** with $NaBAr^F{}_4$ regenerates complex **1**, resulting in the expulsion of **6** from the cavity and reappearance of the ^1H NMR signals for free guest molecule **6**. The cycles of coordination transformations can be repeated with no apparent loss in encapsulation performance (Figure 5).

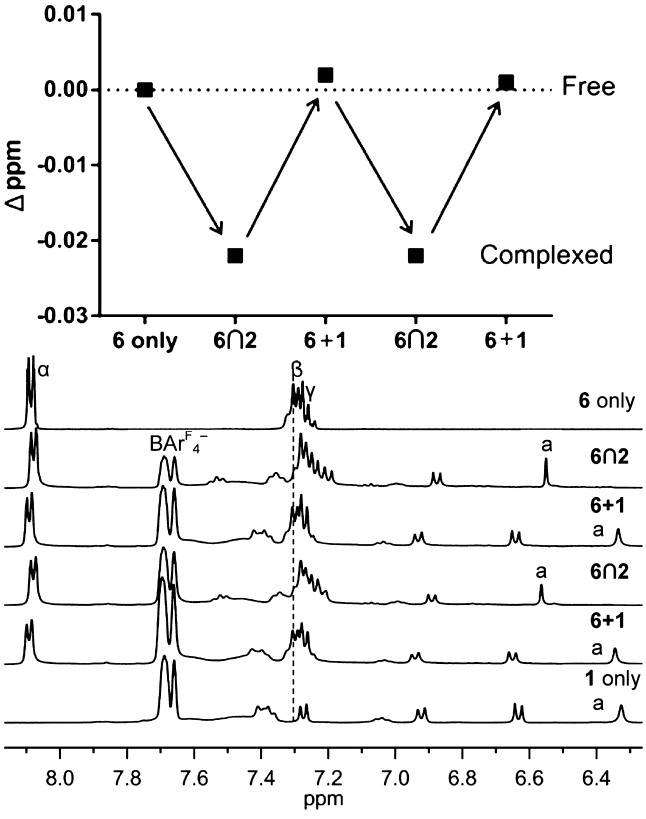

Figure 5. (Top) Allosteric regulation of ion-regulated receptors **1** and **2** demonstrating the ejection and incorporation of guest **6** in CD_3CN. Formation of **1** from **2** was achieved by abstraction of Cl^- with stoichiometric amounts of $NaBAr^F{}_4$. Formation of **2** from **1** was achieved by addition of stoichiometric amounts of tetrabutyl ammonium chloride. (Bottom) ^1H NMR traces in CD_3CN showing the reversible conversion of **2** to **1** in the presence of **6**.

Indeed, the formation of both **1** and **2** corresponds to very rapid processes that are complete within seconds, even after multiple cycles, highlighting the potential of the ion-regulated receptor assembly to be applied in dynamic systems with kinetically fast responses.

Computational Studies. In order to further investigate the orbital origins of the intermolecular interactions that give rise to the selectivity observed in this ion-regulated receptor system, DFT calculations were carried out on the solid-state structures of **6∩2** and **5∩3** with the use of the Gaussian 09, rev D.1[58,59] suite of programs at the B97-D/LANL2DZ level of theory. The selected functional, B97-D, is a density functional of the generalized gradient approximation (GGA) type whose performance in describing noncovalently bound systems, through the inclusion of dispersion effects, has been reported.[60−63] Figure 6 shows the electrostatic potential mapped onto the electron isodensity surface of **6∩2** and **5∩3** in their solid-state structures. The orientation of guests within the cavity correlates with the alignment between high electron density regions and poor electron density. This pattern seems to be particularly important in the case of **6∩2**, where the cationic Pt(II) metal center and the electron-rich calix[4]arene framework generates a total permanent dipole of 19.2 D across the cavity. Guest **6** has a dipole moment of 4.8 D, and its vector is antiparallel with the dipole of the host **2** upon formation of **6∩2**. Host **3** has a much smaller permanent dipole (3.34 D) compared to **2**, and the dipole vector of **5** in host–guest complex **5∩3** is not particularly aligned with the host's dipole.

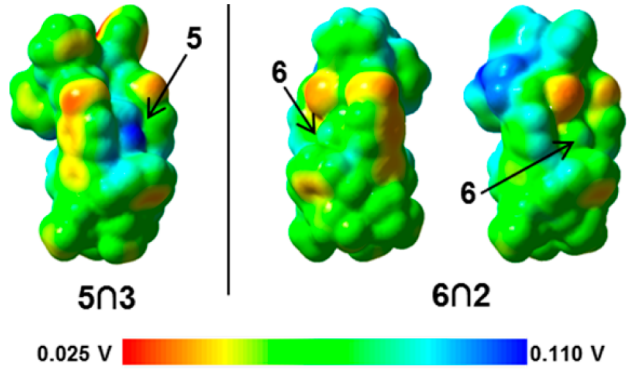

Figure 6. Electrostatic potential map of **5∩3** and **6∩2** showing the charge distribution throughout the inclusion complexes. Regions of high electron density are color coded red, and electron poor regions are blue. Stabilization of host–guest complexes seems to be driven by the interaction of electron-donor and electron-acceptor regions of the complex.

A second-order perturbation analysis on the natural population analysis performed on the X-ray structure of the inclusion complexes assess the most important delocalization interactions between host and guest. In **6∩2**, two interactions between the oxygen atom in **6** and the Pt(II) atom in **2** were observed. First, the lone pairs on the oxygen atom of **6** interact with the lowest virtual natural hybrid orbital on Pt(II) with energies of 2.2 and 1.7 kcal/mol, respectively. A second, slightly weaker interaction (1.43 kcal/mol) was observed between one of the lone pairs on the oxygen atom in **6** and the antibonding orbital of the C–H bond in the ethyl spacer of the P,S ligand. This interaction arises from the excess of electron density on the oxygen atom that is transferred to the neighboring antibonding orbitals. Finally, the bonding orbital between the

dx.doi.org/10.1021/ja503506a | J. Am. Chem. Soc. 2014, 136, 10340−10348

β and γ carbons in guest **6** exhibits a $\pi-\pi$ interaction (1.27 kcal/mol) with the antibonding orbital of the calix[4]arene phenyl ring. Interestingly, in complex **5∩3**, the most significant interactions found were $\pi-\pi$ stacking interactions (1.05 kcal/mol) between the bonding orbital of the calix[4]arene phenyl ring and the antibonding orbital of β and γ carbons in guest of **5**.

CONCLUSION

In summary, we have reported the synthesis and operation of a novel calix[4]arene ion-regulated receptor system assembled via the WLA. By controlling the coordination environment around a Pt(II) regulatory center via the use of small coordinating anions, we have shown that three independent supramolecular configurations can be accessed, each with unique properties based on overall cavity size and charge. Specifically, we have shown that the coordination geometry at the regulatory site dictates the size of the cavity and the nature of the possible electrostatic and dipole interactions, giving rise to selective substrate binding. Crystallographic analysis, NMR spectroscopy, and DFT computational studies shed light on the particular orientations of the guests inside the cavities and the intermolecular forces that dictate the spatial arrangement of the ion-regulated receptor pairs. Finally, we have shown that in situ reversible control of host−guest properties can be achieved by controlling the coordination modes through multiple cycles of chemical inputs. Overall, this work establishes the WLA as a powerful platform for the development of cavitand-based receptors that allow for the design of allosterically regulated enzyme mimics, overcoming some of the assembly limitations that have previously hindered the development of this field.

EXPERIMENTAL SECTION

General Methods. P,S ligand **4** was synthesized and stored using standard Schlenk line conditions, under an inert nitrogen atmosphere. The syntheses of semiopen **2** and closed complex **1** from **4** were performed under inert atmosphere. Transformations between **1**, **2**, and **3** were performed under ambient conditions. *N*-methylpyridinium $BAr^F_4{}^-$ was synthesized and stored in the dark under ambient conditions. All solvents were purchased as HPLC grade and degassed under a stream of argon prior to use. Deuterated solvents were purchased from Cambridge Isotope Laboratories and used as received. Dichloro(1,5-cyclooctadiene) platinum(II), $NaBAr^F_4$, NaCN were purchased from Strem Chemicals, Inc.,and tetrabutyl ammonium chloride was purchased from Aldrich Chemical Co. and used without further purification. Pyridine *N*-oxide was purchased from Aldrich Chemical Co. and subsequently purified by vacuum sublimation. NMR spectra were recorded on a Bruker Avance 400 MHz. ^{1}H NMR spectra were referenced to residual proton resonances in the deuterated solvents. $^{31}P\{^1H\}$ NMR spectra were referenced to an 85% H_3PO_4 aqueous solution in a sealed locker tube. All chemical shifts are reported in ppm. High-resolution mass spectra (HRMS) measurements were recorded on an Agilent 6120 LC-TOF instrument in positive ion mode. Electrospray ionization mass spectra (ESI-MS) were recorded on a Micromas Quatro II triple quadrapole mass spectrometer.

Synthesis. *Closed Ion-Regulated Receptor Complex (1).* Closed complex **1** was prepared under inert atmosphere via the dropwise addition of a solution of hemilabile calix[4]arene ligand **4** (98.3 mg, 0.079 mmol) in 3 mL of CH_2Cl_2 to a suspension of dichloro(1,5-cyclooctadiene) platinum(II) (29.8 mg, 0.079 mmol) in 3 mL of CH_2Cl_2. The solution volume was reduced to approximately 1 mL, and the product was precipitated with pentane. The product was placed in a centrifuge tube, sonicated for 10 min, centrifuged, collected as a precipitate, and washed with pentane. This procedure was repeated three times to afford the dichloride complex species. The closed complex **1** with $BAr^F_4{}^-$ counterions was prepared by dissolving the corresponding chloride complex in 3 mL of CH_3OH in the presence of 2.0 equiv $NaBAr^F_4$ (141.3 mg, 0.158 mmol). The mixture was left to stir for 2 h, followed by solvent evaporation and dissolution in CH_2Cl_2. The NaCl precipitate was removed using a 0.2 μm syringe membrane filter, and the remaining solution was evaporated to afford the corresponding closed complex **1** as a light-yellow solid (107.1 mg, 95%). ^{1}H NMR (400 MHz, 25 °C, CD_2Cl_2) δ 7.79 (s, 16H), 7.64 (d, J = 7.6 Hz, 4H), 7.60 (s, 8H), 7.48 (s, 8H), 7.34−7.21 (m, 12H), 7.04 (t, J = 7.4 Hz, 2H), 6.88 (d, J = 8.1 Hz, 4H), 6.73 (d, J = 8.1 Hz, 4H), 6.37 (s, 4H), 4.60 (d, J = 13.5 Hz, 4H), 4.20−4.14 (m, 4H), 3.77 (t, J = 6.7 Hz, 4H), 3.29 (d, J = 13.6 Hz, 4H), 2.97 (s, broad, 8H), 2.12−1.91 (m, 8H), 1.19 (t, J = 7.4 Hz, 6H), 0.98 (t, J = 7.4 Hz, 6H). $^{31}P\{^1H\}$ NMR (161.98 MHz, 25 °C, CD_2Cl_2): δ 47.1 (J_{P-Pt} = 3052.9 Hz, 2P). HRMS (ESI+) m/z calcd for $C_{80}H_{82}O_4P_2PtS_2$ $[M]^+$: 1427.4777; found: 1427.4728.

Semiopen Ion-Regulated Receptor Complex (2) prepared from 4. Semiopen complex **2** with chloride counterions was prepared in a similar manner as **1**. Under inert atmosphere, a solution of hemilabile calix[4]arene ligand **4** (94.5 mg, 0.076 mmol) in 3 mL of CH_2Cl_2 was added to a suspension of dichloro(1,5-cyclooctadiene) platinum(II) (28.7 mg, 0.076 mmol) in 3 mL of CH_2Cl_2. The solution volume was reduced to approximately 1 mL, and the product was precipitated with pentane. The product was placed in a centrifuge tube, sonicated for 10 min, centrifuged, collected as a precipitate, and washed with pentane. This procedure was repeated three times to yield the dichloride complex species. The semiopen complex **2** with $BAr^F_4{}^-$ counterions was prepared by dissolving the corresponding chloride complex in 3 mL of CH_3OH in the presence of 1.0 equiv $NaBArF_4$ (67.8 mg, 0.076 mmol). The mixture was allowed to stir for **2** hours, followed by solvent evaporation and dissolution in CH_2Cl_2. The NaCl precipitate was removed using a 0.2 μm syringe membrane filter, and the remaining solution was evaporated to afford the corresponding semiopen complex **2** as a yellow solid (174.3 mg, 97%). ^{1}H NMR (400.16 MHz, 25 °C, CD_2Cl_2): δ 7.77 (s, 8H), 7.65−7.56 (m, 8H), 7.53−7.36 (m, 16H), 7.29 (d, J = 7.4 Hz, 4H), 7.08 (t, J = 7.4 Hz, 2H), 6.95 (d, J = 8.0 Hz, 4H), 6.70 (d, J = 7.9 Hz, 4H), 6.38 (s, 4H), 4.58 (d, J = 13.5 Hz, 4H), 4.16 (m, 4H), 3.75 (t, J = 6.6 Hz, 4H), 3.27 (d, J = 13.6 Hz, 4H), 3.12−3.00 (s, 8H), 2.06 (m, 4H), 1.96 (q, J = 7.1 Hz, 4H), 1.18 (t, J = 7.4 Hz, 6H), 0.98 (t, J = 7.4 Hz, 6H).$^{31}P\{^1H\}$ NMR (161.98 MHz, 25 °C, CD_2Cl_2−CD_3OD): δ 50.37 (J_{P-Pt} = 2714.6 Hz, J_{P-P} = 19.2 Hz, 1P), 7.10 (J_{P-Pt} = 3349.1 Hz, J_{P-P} = 19.2 Hz, 1P). HRMS (ESI+) m/z calcd for $C_{80}H_{82}ClO_4P_2PtS_2$ $[M + H]^+$: 1463.4466; found: 1463.4494.

Fully Open Ion-Regulated Receptor Complex (3) prepared from 4. Fully open complex **3** was prepared in a similar manner as **1**. Under inert atmosphere via a solution of hemilabile calix[4]arene ligand **4** (161.6 mg, 0.131 mmol) in 3 mL of CH_2Cl_2 was added to a suspension of dichloro(1,5-cyclooctadiene) platinum(II) (49.0 mg, 0.131 mmol) in 3 mL of CH_2Cl_2. The solution volume was reduced to approximately 1 mL, and the product was precipitated with pentane. The product was placed in a centrifuge tube, sonicated for 10 min, centrifuged down, and washed with pentane. This procedure was repeated three times to afford the dichloride complex species. Fully open complex was prepared by, dropwise addition of NaCN in CH_3OH (0.146 M, 0.625 mL, 0.095 mmol) into a 4 mL 1:1 CH_2Cl_2−CH_3OH solution of the dichloride complex (71.2 mg, 0.047 mmol). The mixture was left to stir for 2 h, followed by solvent evaporation and dissolution in CH_2Cl_2 upon gentle heating. The NaCl precipitate was removed using a 0.2 μm syringe membrane filter, and the remaining solution was evaporated to afford the corresponding closed complex as a white solid (182.4 mg, 94%). ^{1}H NMR (400.16 MHz, 25 °C, CD_2Cl_2): δ 7.84−7.64 (m, 8H), 7.62−7.48 (m, 12H), 7.23 (d, J = 7.4 Hz, 4H), 7.02 (d, J = 8.2 Hz, 4H), 6.71 (d, J = 8.3 Hz, 4H), 6.45 (s, 4H), 4.56 (d, J = 13.0 Hz, 4H), 4.17 (m, 4H), 3.73 (t, J = 6.8 Hz, 4H), 3.28−3.21 (m, 12H), 2.13 (m, 4H), 1.97 (m, 4H), 1.16 (t, J = 7.4 Hz, 6H), 0.98 (t, J = 7.5 Hz, 6H). $^{31}P\{^1H\}$ NMR (161.98 MHz, 25 °C, CD_2Cl_2): δ 8.35 (J_{P-Pt} = 2176.9 Hz, 2P). HRMS (ESI+) m/z calcd for $C_{82}H_{82}N_2O_4P_2PtS_2$ $[M + Na]^+$: 1503.6848; found: 1503.4781.

dx.doi.org/10.1021/ja503506a | J. Am. Chem. Soc. 2014, 136, 10340−10348

*Fully Open Ion-Regulated Receptor Complex (**3**) from **1** or **2**.* Fully open complex **3** was prepared under ambient conditions by dropwise addition of 2.0 equiv of NaCN in CH_3OH (0.146 M, 0.625 mL, 0.095 mmol) into a 4 mL 1:1 CH_2Cl_2-CH_3OH solution of complex **1** or **2** (1.0 equiv, 0.047 mmol). The mixture was left to stir for 2 h, followed by solvent evaporation and dissolution in CH_2Cl_2 upon gentle heating. The NaCl precipitate was removed using a 0.2 μm syringe membrane filter, and the remaining solution was evaporated to afford the corresponding closed complex as a white solid (132.2 mg, 94%). ^{1}H NMR (400.16 MHz, 25 °C, CD_2Cl_2): δ 7.84−7.64 (m, 8H), 7.62−7.48 (m, 12H), 7.23 (d, J = 7.4 Hz, 4H), 7.02 (d, J = 8.2 Hz, 4H), 6.71 (d, J = 8.3 Hz, 4H), 6.45 (s, 4H), 4.56 (d, J = 13.0 Hz, 4H), 4.17 (m, 4H), 3.73 (t, J = 6.8 Hz, 4H), 3.28−3.21 (m, 12H), 2.13 (m, 4H), 1.97 (m, 4H), 1.16 (t, J = 7.4 Hz, 6H), 0.98 (t, J = 7.5 Hz, 6H). ^{31}P{^{1}H} NMR (161.98 MHz, 25 °C, CD_2Cl_2): δ 8.35 (J_{P-Pt} = 2176.9 Hz, 2P). HRMS (ESI+) m/z calcd for $C_{82}H_{82}N_2O_4P_2PtS_2$ $[M + Na]^+$: 1503.6848; found: 1503.4781.

In Situ Reversibility Betweem Ion-Regulated Receptor Complex 1 and 2. In a capped airtight NMR tube, semiopen complex **2** (20.0 mg, 0.0086 mmol) and guest **6** (5.7 mg, 0.0601 mmol) were dissolved in 2 mL of CD_3CN. The sample was shaken and analyzed immediately via NMR spectroscopy. Semiopen complex **2** was converted to closed complex **1** by addition of 1.0 equiv of $NaBAr^F_4$ (38 μL, 0.225 M, 0.0086 mmol) as a CD_3CN solution to the solution containing **2** and **6** and vigorously shaking the sample. Closed complex **1** was reverted to semiopen complex **2** by addition of 1.0 equiv of tetrabutyl ammonium chloride (30 μL, 0.288 M, 0.0086 mmol) as a CD_3CN solution to the solution of **1** and **6** and vigorously shaking the sample. The reversible process was repeated for two full cycles, and precipitation of NaCl was visible after the end of the cycle (in situ ^{1}H NMR yields = quantitative).

X-ray Crystallography. Crystallographic data are displayed in the Supporting Information. Crystals suitable for X-ray diffraction of **1** were grown by slow diffusion of *n*-pentane into a solution of **1** in 1,2-dichloroethane. Crystals of **6∩2** and **5∩3** were grown by slow diffusion of pentane into a 1:1 guest−host solution in 1,2-dichloroethane. Single crystals of **1**, **6∩2**, and **5∩3** were mounted in inert oil (Infineum V8512) and transferred to the cold nitrogen gas stream of a Bruker Kappa APEX CCD diffractometer equipped with a CuKα microsource with Quazar optics (**1**, **6∩2**) or a MoKα sealed tube with a graphite monochromator (**5∩3**). Data were processed using APEX2 from Bruker, and a multiscan absorption correction was applied using SADABS. Structures for **1** and **5∩3** were solved using dual space methods; **6∩2** was solved using direct methods. Non-hydrogen atoms were refined anisotropically. Hydrogen atoms were included in idealized positions but not refined. Their positions and isotropic displacement parameters were restrained relative to their parent atoms.

■ ASSOCIATED CONTENT

Supporting Information

Synthetic procedures, spectral data, titration studies, Job plots, binding affinity data, computational details, and crystallographic data for **1**, **6∩2**, **5∩3**. This material is available free of charge via the Internet at http://pubs.acs.org.

■ AUTHOR INFORMATION

Corresponding Author

chadnano@northwestern.edu

Notes

The authors declare no competing financial interest.

■ ACKNOWLEDGMENTS

This material is based upon work supported by the following awards, National Science Foundation CHE-1149314, U.S. Army W911NF-11-1-0229. J.M.A. acknowledges a fellowship from Consejo Nacional de Ciencia y Tecnologia (CONACYT) and J.B.F. is grateful to DGAPA−UNAM contract IB200313 and DGCTIC−UNAM for granting access to their computing facilities.

■ REFERENCES

(1) Saibil, H. R.; Fenton, W. A.; Clare, D. K.; Horwich, A. L. *J. Mol. Biol.* **2013**, *425*, 1476−1487.
(2) Perutz, M. F. *Nature* **1970**, *228*, 726−739.
(3) Monod, J.; Changeux, J. P.; Jacob, F. *J. Mol. Biol.* **1963**, *6*, 306−329.
(4) Hartl, F. U. *Nat. Med.* **2011**, *17*, 1206−1210.
(5) Hartl, F. U.; Bracher, A.; Hayer-Hartl, M. *Nature* **2011**, *475*, 324−332.
(6) Tang, Y. C.; Chang, H. C.; Roeben, A.; Wischnewski, D.; Wischnewski, N.; Kerner, M. J.; Hartl, F. U.; Hayer-Hartl, M. *Cell* **2006**, *125*, 903−914.
(7) Perutz, M. F. *Annu. Rev. Physiol.* **1990**, *52*, 1−25.
(8) Perutz, M. F.; Wilkinson, A. J.; Paoli, M.; Dodson, G. G. *Annu. Rev. Biophys. Biomol. Struct.* **1998**, *27*, 1−34.
(9) Azov, V. A.; Beeby, A.; Cacciarini, M.; Cheetham, A. G.; Diederich, F.; Frei, M.; Gimzewski, J. K.; Gramlich, V.; Hecht, B.; Jaun, B.; Latychevskaia, T.; Lieb, A.; Lill, Y.; Marotti, F.; Schlegel, A.; Schlittler, R. R.; Skinner, P. J.; Seiler, P.; Yamakoshi, Y. *Adv. Funct. Mater.* **2006**, *16*, 147−156.
(10) Gottschalk, T.; Jaun, B.; Diederich, F. *Angew. Chem., Int. Ed. Engl.* **2007**, *46*, 260−264.
(11) Maslak, V.; Yan, Z.; Xia, S.; Gallucci, J.; Hadad, C. M.; Badjic, J. D. *J. Am. Chem. Soc.* **2006**, *128*, 5887−5894.
(12) Kang, S. W.; Castro, P. P.; Zhao, G.; Nunez, J. E.; Godinez, C. E.; Gutierrez-Tunstad, L. M. *J. Org. Chem.* **2006**, *71*, 1240−1243.
(13) Wang, Q.-C.; Qu, D.-H.; Ren, J.; Chen, K.; Tian, H. *Angew. Chem., Int. Ed.* **2004**, *43*, 2661−2665.
(14) Mulder, A.; Jukovic, A.; Lucas, L. N.; van Esch, J.; Feringa, B. L.; Huskens, J.; Reinhoudt, D. N. *Chem. Commun. (Cambridge, U. K.)* **2002**, 2734−2735.
(15) Berryman, O. B.; Sather, A. C.; Rebek, J., Jr. *Chem. Commun. (Cambridge, U. K.)* **2011**, *47*, 656−658.
(16) Letzel, M. C.; Schafer, C.; Novara, F. R.; Speranza, M.; Rozhenko, A. B.; Schoeller, W. W.; Mattay, J. *J. Mass. Spectrom.* **2008**, *43*, 1553−1564.
(17) Pochorovski, I.; Boudon, C.; Gisselbrecht, J. P.; Ebert, M. O.; Schweizer, W. B.; Diederich, F. *Angew. Chem., Int. Ed. Engl.* **2012**, *51*, 262−266.
(18) Frei, M.; Diederich, F.; Tremont, R.; Rodriguez, T.; Echegoyen, L. *Helv. Chim. Acta* **2006**, *89*, 2040−2057.
(19) Pochorovski, I.; Ebert, M. O.; Gisselbrecht, J. P.; Boudon, C.; Schweizer, W. B.; Diederich, F. *J. Am. Chem. Soc.* **2012**, *134*, 14702−14705.
(20) Fox, O. D.; Dalley, N. K.; Harrison, R. G. *J. Am. Chem. Soc.* **1998**, *120*, 7111−7112.
(21) Zuccaccia, D.; Pirondini, L.; Pinalli, R.; Dalcanale, E.; Macchioni, A. *J. Am. Chem. Soc.* **2005**, *127*, 7025−7032.
(22) Pluth, M. D.; Bergman, R. G.; Raymond, K. N. *Acc. Chem. Res.* **2009**, *42*, 1650−1659.
(23) Yoshizawa, M.; Klosterman, J. K.; Fujita, M. *Angew. Chem., Int. Ed.* **2009**, *48*, 3418−3438.
(24) Yoon, H. J.; Mirkin, C. A. *J. Am. Chem. Soc.* **2008**, *130*, 11590−11591.
(25) Kuwabara, J.; Stern, C. L.; Mirkin, C. A. *J. Am. Chem. Soc.* **2007**, *129*, 10074−10075.
(26) Staats, H.; Eggers, F.; Hass, O.; Fahrenkrug, F.; Matthey, J.; Luning, U.; Lutzen, A. *Eur. J. Org. Chem.* **2009**, 4777−4792.
(27) Eisenberg, A. H.; D, F. M.; Mirkin, C. A.; Stern, C. L.; Incarvito, C. D.; Rheingold, A. L. *Organometallics* **2001**, *20*, 2052−2058.
(28) Holliday, B. J.; Mirkin, C. A. *Angew. Chem., Int. Ed.* **2001**, *40*, 2022−2043.
(29) Chakrabarty, R.; Mukherjee, Partha S.; Stang, P. J. *J. Chem. Rev.* **2011**, *111*, 6810−6918.
(30) Kremer, C.; Lutzen, A. *Chem.—Eur. J.* **2013**, *19*, 6162−6196.

(31) Yamanaka, M.; Kawaharada, M.; Nito, Y.; Takaya, H.; Kobayashi, K. *J. Am. Chem. Soc.* **2011**, *133*, 16650−16656.
(32) Cacciarini, M.; Azov, V. A.; Seiler, P.; Kunzer, H.; Diederich, F. *Chem. Commun. (Cambridge, U. K.)* **2005**, 5269−5271.
(33) Gibb, C. L.; Gibb, B. C. *J. Am. Chem. Soc.* **2004**, *126*, 11408−11409.
(34) Yoshizawa, M.; Sato, N.; Fujita, M. *Chem. Lett.* **2005**, *34*, 1392−1393.
(35) Javor, S.; Rebek, J., Jr. *J. Am. Chem. Soc.* **2011**, *133*, 17473−17478.
(36) Hooley, R. J.; Biros, S. M.; Rebek, J., Jr. *Angew. Chem., Int. Ed. Engl.* **2006**, *45*, 3517−3519.
(37) Kubitschke, J.; Javor, S.; Rebek, J., Jr. *Chem. Commun. (Cambridge, U. K.)* **2012**, *48*, 9251−9253.
(38) Ryan, D. A.; Rebek, J., Jr. *J. Am. Chem. Soc.* **2011**, *133*, 19653−19655.
(39) Gianneschi, N. C.; Masar, M. S., III; Mirkin, C. A. *Acc. Chem. Res.* **2005**, *38*, 825−837.
(40) Wiester, M. J.; Ulmann, P. A.; Mirkin, C. A. *Angew. Chem., Int. Ed.* **2011**, *50*, 114−137.
(41) Kennedy, R. D.; Machan, C. W.; McGuirk, C. M.; Rosen, M. S.; Stern, C. L.; Sarjeant, A. A.; Mirkin, C. A. *Inorg. Chem.* **2013**, *52*, 5876−5888.
(42) Lifschitz, A. M.; Shade, C. M.; Spokoyny, A. M.; Mendez-Arroyo, J.; Stern, C. L.; Sarjeant, A. A.; Mirkin, C. A. *Inorg. Chem.* **2013**, *52*, 5484−5492.
(43) Masar, M. S., III; Gianneschi, N. C.; Oliveri, C. G.; Stern, C. L.; Nguyen, S. T.; Mirkin, C. A. *J. Am. Chem. Soc.* **2007**, *129*, 10149−10158.
(44) Yoon, H. J.; Kuwabara, J.; Kim, J. H.; Mirkin, C. A. *Science (Washington, U. S.)* **2010**, *330*, 66−69.
(45) *Calixarenes 2001*; Asfari, Z., Bohmer, V., Harrowfield, J., Vicens, J., Eds.; Kluwer Academic Publishers: Dordrecht, The Netherlands, 2001.
(46) *Calixarenes and Resorcinarenes Synthesis, Properties and Applications*; Sliwa, W., Kozlowski, C., Eds.; Wiley-VCH: Weinheim, Germany, 2009.
(47) Gutsche, C. D. *Calixarenes: An Introduction (Monograms in Supramolecular Chemistry)*, 2nd ed.; Stoddart, J. F., Ed.; The Royal Society of Chemistry: Cambridge, U.K., 2008.
(48) Araki, K.; Hisaichi, K.; Kanai, T.; Shinkai, S. *Chem. Lett.* **1995**, *24*, 569−570.
(49) Rosen, M. S.; Stern, C. L.; Mirkin, C. A. *Chem. Sci.* **2013**, *4*, 4193−4198.
(50) Yoo, H.; Rosen, M. S.; Brown, A. M.; Wiester, M. J.; Stern, C. L.; Mirkin, C. A. *Inorg. Chem.* **2012**, *51*, 11986−11995.
(51) Araki, K.; Shimizu, H.; Shinkai, S. *Chem. Lett.* **1993**, *22*, 205−208.
(52) Inokuchi, F.; Araki, K.; Shinkai, S. *Chem. Lett.* **1994**, *23*, 1383−1386.
(53) Arduini, A.; M, M.; Paganuzzi, D.; Pochini, A.; Secchi, A.; Ugozzoli, F.; Ungaro, R. *J. Chem. Soc., Perkin Trans. 2* **1996**, 839−846.
(54) Steed, J. W.; Johnson, C. P.; Barnes, C. L.; Juneja, R. K.; Atwood, J. L.; Reilly, S.; Hollis, R. L.; Smith, P. H.; Clark, D. L. *J. Am. Chem. Soc.* **1995**, *117*, 11426−11433.
(55) Arduini, A.; Pochini, A.; Secchi, A. *Eur. J. Org. Chem.* **2000**, 2325−2334.
(56) Ross, H.; Luning, U. *Angew. Chem., Int. Ed. Engl.* **1995**, *34*, 2555−2557.
(57) Yoshimura, K.; Fukazawa, Y. *Tetrahedron Lett.* **1996**, *37*, 1435−1438.
(58) Frisch, M. J.; Trucks, G. W.; Schlegel, H. B.; Scuseria, G. E.; Robb, M. A.; Cheeseman, J. R.; Scalmani, G.; Barone, V.; Mennucci, B.; Petersson, G. A.; Nakatsuji, H.; Caricato, M.; Li, X.; Hratchian, H. P.; Izmaylov, A. F.; Bloino, J.; Zheng, G.; Sonnenberg, J. L.; Hada, M.; Ehara, M.; Toyota, K.; Fukuda, R.; Hasegawa, J.; Ishida, M.; Nakajima, T.; Honda, Y.; Kitao, O.; Nakai, H.; Vreven, T.; Montgomery, J. A., Jr.; Peralta, J. E.; Ogliaro, F.; Bearpark, M.; Heyd, J. J.; Brothers, E.; Kudin, K. N.; Staroverov, V. N.; Kobayashi, R.; Normand, J.; Raghavachari, K.; Rendell, A.; Burant, J. C.; Iyengar, S. S.; Tomasi, J.; Cossi, M.; Rega, N.; Millam, N. J.; Klene, M.; Knox, J. E.; Cross, J. B.; Bakken, V.; Adamo, C.; Jaramillo, J.; Gomperts, R.; Stratmann, R. E.; Yazyev, O.; Austin, A. J.; Cammi, R.; Pomelli, C.; Ochterski, J. W.; Martin, R. L.; Morokuma, K.; Zakrzewski, V. G.; Voth, G. A.; Salvador, P.; Dannenberg, J. J.; Dapprich, S.; Daniels, A. D.; Farkas, Ö.; Foresman, J. B.; Ortiz, J. V.; Cioslowski, J.; Fox, D. J. *Gaussian 09*, revision D.01; Gaussian, Inc.: Wallingford, CT, 2010
(59) Glendening, E. D. Reed, A. E.; Carpenter, J. E.; Weinhold, F. *NBO*, version 3.1; Gaussian, Inc.: Wallingford, CT, 2010.
(60) Hay, P. J.; Wadt, W. R. *J. Chem. Phys.* **1985**, *82*, 270−283.
(61) Cundari, T. R.; Benson, M. T.; Lutz, M. L.; Sommerer, S. O. *Rev. Comput. Chem.* **1996**, *8*, 145−202.
(62) Muck-Lichtenfeld, C.; Grimme, S.; Kobryn, L.; Sygula, A. *Phys. Chem. Chem. Phys.* **2010**, *12*, 7091−7097.
(63) Josa, D.; Rodriguez Otero, J.; Cabaleiro Lago, E. M. *Phys. Chem. Chem. Phys.* **2011**, *13*, 21139−21145.